

# The CHARA Array

## Center for High Angular Resolution Astronomy of Georgia State University

Mount Wilson Observatory

Mount Wilson, California, 91023 USA

## CLASICC/CLIMB++: What should it be?

CHARA Technical Report #103

Theo ten Brummelaar - Marc-Antoine Martinod – Peter Tuthill

Version 2: 2020-10-21

### 1.0 INTRODUCTION

This technical report is intended to aid in the decision-making process for the basic design of the upgrade to the CLASSIC/CLIMB (CC) beam combiner. We call the new combiner CC++. The primary aim of this upgrade is to achieve the best possible sensitivity for visibility and phase closure measurements on at least one baseline triad. Every other design consideration, apart from physical and cost limitations, is secondary to that. This means that the AO system will at best be able to correct for slow changes of aberrations in the optical system and will not be correcting for atmospheric turbulence.

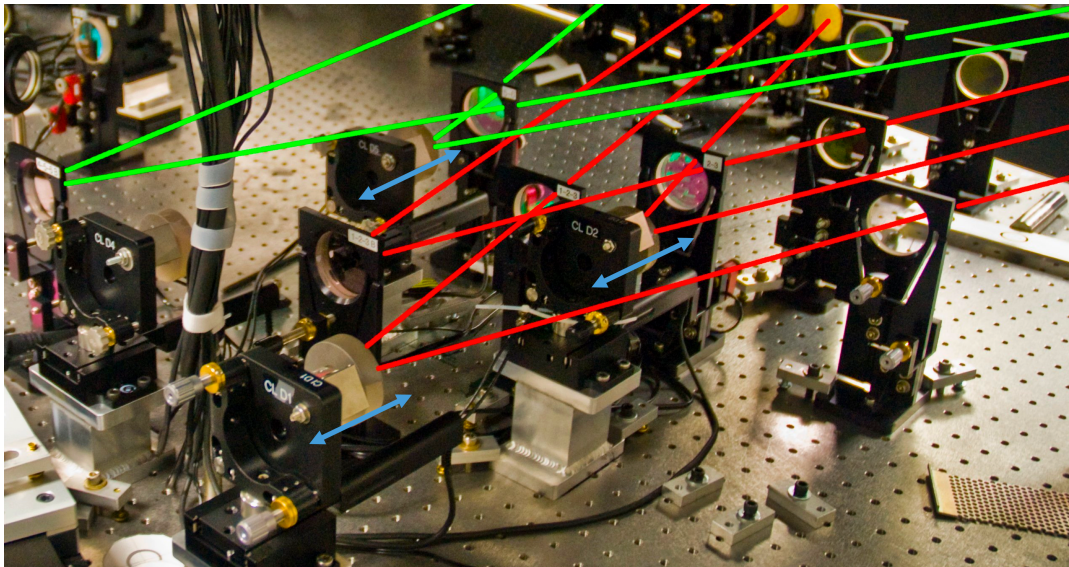


**Figure 1.** The CLASSIC (Top) and CLIMB (Bottom) beam combiners. The beam locations are drawn in green and red, respectively. The “dither mirrors” modulate the path-length of one beam by up to 150  $\mu\text{m}$  as indicated by the blue directional arrows. The two beam CLASSIC can be reconfigured to form a second three-way CLIMB combiner.

We also assume that we will be, for the very faintest objects, relying on the astrometric model to keep the fringe packet within a usable part of delay space.

The current CLIMB/CLASSIC combiner (Figure 1) is an aperture plane temporal encoding scheme where the beams are combined on bulk optics and then fed onto single pixels on the PICNIC detector with no spectral dispersion within the band. While the original proposal only spoke to a simple upgrade of the detector system, we thought it best to also consider the alternative design of an image plane detector scheme with three beams in a non-redundant pattern along with spectral dispersion.

The question we'd like to answer is: does one design have an intrinsic advantage over the other from the point of view of signal to noise?

## 2.0 INPUT PARAMETERS

Here we set out the basic parameters of each combiner with the intent of ensuring the comparison is as fair as possible in the sense that they have the same or range of delay space error allowed, field of view, and integration time.

### 2.1 Photometric Model

Developed for the original proposal, the photometric model is empirical and based on observations taken during 2017 and 2018 with the CLASSIC beam combiner (Figure 2.). All these data were obtained using the default sample rate of 750 Hz.

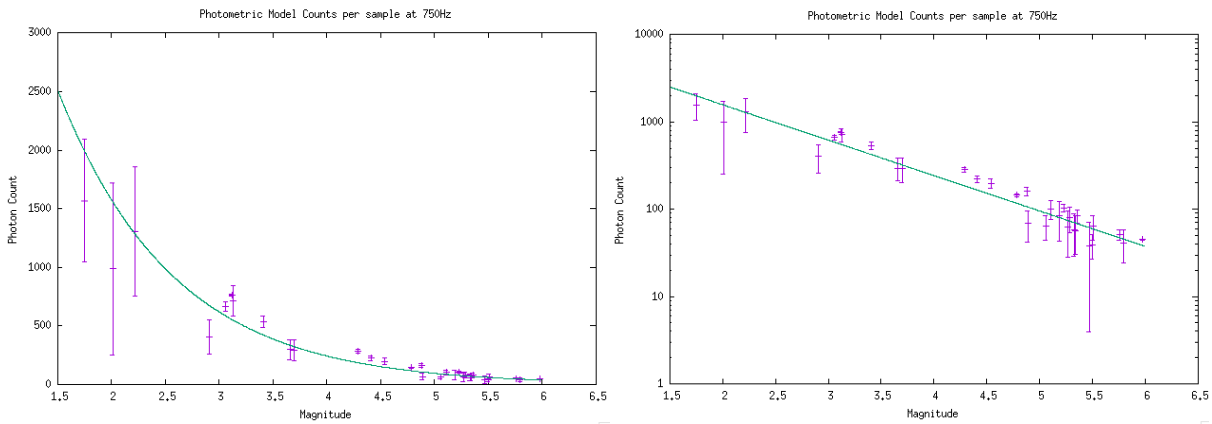


**Figure 2.** Plots of The photometric model used in the original proposal. On left the data are shown on a linear plot and on the right on a logarithmic plot.

The empirical fit found, and used for the proposal, is

$$N_{ph} = 10189 \times e^{-M/1.071}$$

where  $M$  is the magnitude of the star in question, and  $N$  is the number of counts received in a single exposure on a single pixel at 750 Hz. An empirical model was used due to the many non-linear effects on the total count. For example while there is the raw optical throughput of the system there is also the current weather conditions and optical depth of the atmosphere to take into account. Added to that the field of view of a single pixel is fixed, while the seeing disk size is not and the response of the detector is non-linear for very high count rates. Finally, there are always small alignment drifts during a full data sequence, as well as small differences in alignment from evening to evening.

## 2.2 Field of view

The pixel size of the current system is 0.78 arcseconds on the sky. This was based on modeling we did at the time of construction that showed that this was the optimum pixel size for K band. Since we expect to operate the new system in both K and H band, we will continue to use this size for a single pixel for the aperture plane design and set the field of view of the image plane system to one Airy disk.

## 2.3 Number of Pixels for Aperture Plane Design

In the case of the aperture plane design the number of samples in a single scan is

$$N_{Ap} = L / \Delta L_{Ap}$$

where  $\Delta L_{Ap}$  is the amount of delay space covered in a single sample and  $L$  is the length of the scan. We have found that the smallest number of samples per fringe required to produce data that calibrates well is just above Nyquist at 3 samples per wavelength  $\lambda$ . For three baselines we encode the fringes at three frequencies  $f$ ,  $2f$ , and  $3f$ . So, in order to adequately sample the highest fringe frequency, we need to have

$$\Delta L_{Ap} = \frac{\lambda}{9}$$

which gives us

$$N_{Ap} = \frac{9L}{\lambda}$$

The maximum length of the scan is set by the PZT actuators we use and is currently 100 $\mu$ m so in H band we have 538 samples per scan at  $F_{Ap} = 750$  Hz, or a sample time of  $T_{Ap} = 1.33$  mS. The fringes will be encoded at 250, 166.7, and 83.3 Hz.

One full scan will take  $N_{Ap} T_{Ap}$  which in this example will be 0.72 S.

In H band the fringe packet is about 20  $\mu$ m across, so we will spend at most only 20% of the total scan actually looking at fringes, the rest will be noise<sup>1</sup>.

The photometry per pixel for the aperture plane design is  $N_{ph}$  as described in section 2.1.

Note that in the case of CLASSIC we have two output streams and in CLIMB we have three. These can be combined to form a single output stream.

## 2.4 Number of Pixels for Image Plane Design

The fringe spacing of the image plane design is determined by the layout of the incoming beams. The minimum distance is a linear spacing of  $1D$ ,  $2D$ , and  $3D$  where  $D$  is the diameter of the beam. However, for such close spacing there will be speckle contamination and other cross talk due to seeing, so we set the spacing at  $2D$ ,  $4D$ , and  $6D$ . The number of fringes across the Airy disk will be  $2.44 \times N$  so we will have 4.88, 9.76 and 14.64. Rounding up this means a minimum of  $3 \times 15 = 45$  pixels across the Airy disk, less for across the FOV.

---

<sup>1</sup> It is at this point that the good Dr. Tuthill will point out that he has been saying this all along.

The amount of spectral dispersion

$$R = \frac{\lambda}{\Delta\lambda}$$

is then determined by the required delay range

$$L = \frac{2\lambda^2}{\Delta\lambda}$$

where the factor of 2 is included as we can go a full coherence length either side of the zero-delay position and still know where the fringes are. Thus, we get

$$R = \frac{L}{2\lambda}$$

which in our case will be 30. This gives us a bandwidth of 0.056  $\mu\text{m}$  for each channel and  $0.285/0.056 = 5$  pixels across the H band. The number of pixels required for each sample is then  $N_{Im} = 5 \times 45 = 225$ .

In the current CLASSIC/CLIMB reduction package we calculate the triple product in each 9-pixel segment of the scan, or one wavelength of the slowest fringe. We can, therefore, set the sample rate of the image plane system to  $F_{Im} = \frac{F_{Ap}}{9} = 83.33$  Hz or a sample time to  $T_{Im} = 12$  mS. In order to look for fringes we can incoherently integrate these samples over the same time as it takes the aperture plane system to complete one scan, in our case 0.72 S or 60 samples.

The photometry per pixel for the image plane design will be  $\frac{9N_{ph}}{225} = 0.04 N_{ph}$ .

### **3.0 CAMERA SPECIFICATION**

The manufacturer's specification on their web site states that the readout noise at 3500 FPS and a gain of 20 is  $< 1 e^-$ , but reports from MircX and ANU give  $0.7 e^-$ , so we will use this. The excess noise factor is quoted as 1.25 and there is no evidence at hand to conflict with this. The dark current is quoted as  $< 80 e^- p^{-1} S^{-1}$ . Recent data from First Light give a value of 50 for dark noise. The difficulty here is that reports of the older cameras state that this was present all the time, independent of the input, so in order to be conservative we will assume this is present in both H and K bands. K band will also be subject to background noise from the outside environment. The quantum efficiency is stated to be  $> 60\%$ , however this is taken into account in the empirical photometric model in section 2.1 and need not be included twice.

### **4.0 SIMULATIONS**

The final input parameters to be used in the simulations are set out in Table 1 below. Simulations were run using both the current CLIMB design using the aperture plane and for a three-beam image plane design. The simulations were carried out by Marc-Antoine Martinod at the University of Sydney.

**Table 1: Input Parameters**

Parameter	Aperture Plane Design	Image Plane Design
Readout Rate	750 Hz	83.3 Hz
Sample Time	1.33 mS	12 mS
Photometry per pixel	$N_{ph}$	$0.04 N_{ph}$
Delay Range	$\pm 50 \mu\text{m}$	$\pm 50 \mu\text{m}$
Spectral Dispersion R	1	30
Central Wavelength	$1.673 \mu\text{m}$	$1.673 \mu\text{m}$
Bandwidth Per Channel	$0.285 \mu\text{m}$	$0.056 \mu\text{m}$
Number of Spectral Channels	1	5
Number pixels across fringes.	3-6-9	5-10-15
Pixels read per sample	1	225
Field of View	$3.78 \mu\text{rad}$	Airy Disk
Integration Time	0.72 S	0.72 S
Samples per integration	538	60
Total pixels per integration	538	13500
Camera Read Noise	$0.7 e^-$	$0.7 e^-$
Camera Dark Current	$50 e^- p^{-1} S^{-1}$	$50 e^- p^{-1} S^{-1}$
Camera Excess Noise Factor	1.25	1.25

#### **4.1 Description of the simulations**

There is one simulation per design: pupil plane combiner and image plane combiner. The simulations are run 100 times to get a reliable measurement of the SNR, notably at low flux. It represents an 8-hour computation time for the pupil plane combiner and 20s for the image plane combiner despite the use of GPU to accelerate the execution. Each simulation has four parts:

**Creation of a phase mask representing the atmosphere across each pupil:** Phase masks are the same for both simulations. Fringe blurring is simulated by translating the phase mask during a scan for the pupil plane combiner, by oversampling in time the duration of the acquisition of one frame for the image combiner. During the translation of the mask, any pixel on one edge is wrapped around to the other side. The phase mask is ten times larger than the size of one pupil to avoid any periodic effect due to the wrapping. Wraparound caused noticeable artefacts in the temporal scan in the early development of the simulation. With this larger screen no wrapping effects occur. To reproduce a visibility of 0.75 in K band, we set an  $r_0$  of 3.35 cm and a wind speed of 15 m/s.

**Simulation of the combiner and the corresponding interferometric signal:** The simulation of the pupil plane combiner is based on the description of CLASSIC made in the article “The CLASSIC/climb Beam Combiner at the CHARA Array” (ten Brummelaar, 2013).

The simulation of the image plane combiner is based on the numbers derived in the previous sections: recombination according to the configuration 2-4-6D (D=size of the pupil) and spectral dispersion (See Figure 3).

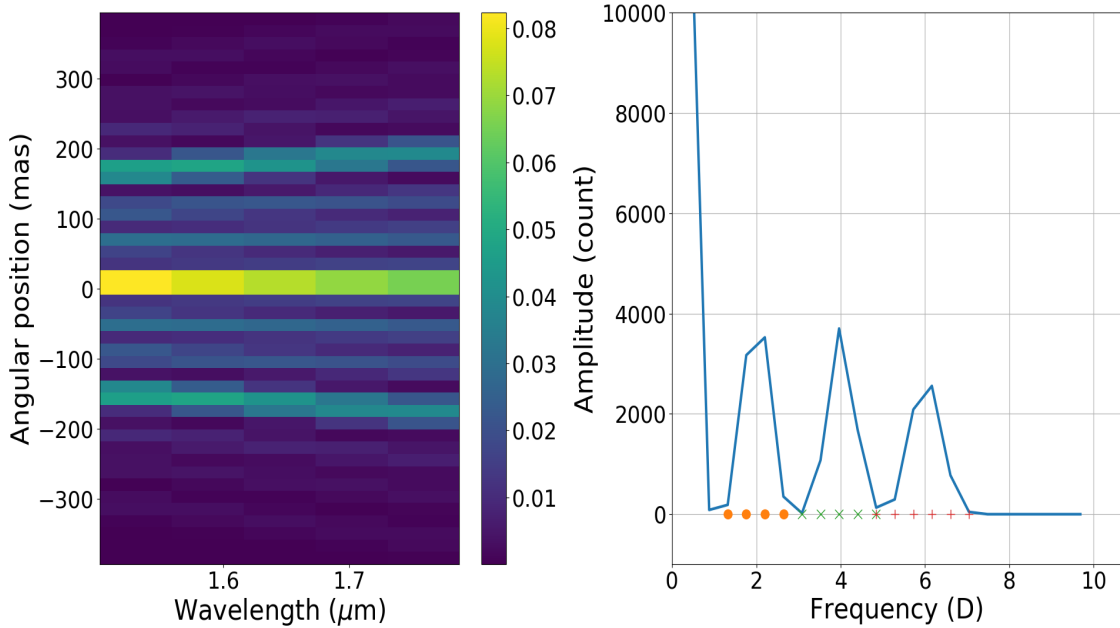


**Figure 3.** Left: noise-free and turbulence-free interferogram. Right: Slice of the 2D-DSP showing the three fringe-peaks. Dotted lines represent the width of integration along the spatial axis. We can also see some cross-talk due to the bandwidth. Turbulence may increase that if speckles arise (speculating thoughts).

**Adding detector noise onto the signal:** The detector is the C-Red One camera. In the case of the pupil plane, the full array of pixels is created. Given the plate scale of CLASSIC, the signal is projected on one pixel per output of the combiner. Thus, one pixel per output is read.

In the case of the image plane combiner, only the read pixels are created: an array of 45 per 5 pixels to avoid saturation of the memory and excessive execution time.

The simulated noises are the photon noise, the dark noise, the excess noise factor and the read-out noise. The first three noises are added to the signal as follow:

$$noisy\ frames = noise - free\ frames + N(0, sig)$$

With

$$sig = \sqrt{(noise - free\ frame + dark) ENF}$$

and  $N$  is the normal distribution. We should have used a Poisson distribution, but had to consider the ENF. A Gamma distribution should represent the amplification process, but the delivered signal has an ENF of 2, which is the maximum value in any amplification process in EMCCD or e-APD if no effort

is put to dim this effect as far as we know. For the sake of simplicity and efficiency, we chose the solution above, also used by other teams owning a C-Red One.

On top of the noisy frame, the read noise is added as a Gaussian noise of mean 0 and a sigma equal to the read-out noise.

**Extraction of the fringe-peak and measurement of its SNR:** The measurement of the fringe-peak in the pupil plane combiner follows the instruction in the article cited above: normalization then the combination of the outputs, Fourier transform and measurement. The width on which a fringe-peak is integrated is analytically defined so that

$$width = \lambda_0 \times \Delta\sigma \times f,$$

with  $\lambda_0$  the central wavelength,  $\Delta\sigma$  the bandwidth in wavenumber and  $f$  the temporal frequency of the fringes. The width of the fringe-peak depends on the speed of the scan (frequency of encoding  $f$ ) and the inverse of the number of fringes in the envelope ( $\lambda_0 \times \Delta\sigma$ ).

In the case of the image plane combiner, the 2D-Fourier transform of the dispersed fringes is done. We chose a 2D-FT because it gives the best sensitivity compared to a 1D-FT per spectral channel which are summed together. The SNR of the former is proportional to the squared number of photons in all your spectral channels divided by the noise:

$$(N_{channel} \times \frac{N_{photon}}{noise})^2.$$

The SNR of the latter evolves as

$$N_{channel} \times (\frac{N_{photon}}{noise})^2.$$

Consequently, the SNR of the 2D-FT is  $N_{channel}$  higher than the SNR of the 1D-FT. The counterpart is that the fringe-peaks are more likely to have cross-talk as the 2D-FT (Fig. 3, right) is done on a larger bandwidth than in a 1D-FT for which the bandwidth per FT is one spectral channel, even before considering the atmosphere turbulence. It is the case here, but it is negligible. Reducing the bandwidth or increase the space between the pupils removes the cross-talk.

The fringe-peak is integrated along the whole horizontal width of the FT, the width in the spatial frequency is defined by

$$width = \frac{f}{\lambda_{min}} \lambda_0 + \Delta f - \frac{f}{\lambda_{max}} \lambda_0 - \Delta f$$

so that  $f$  is the fringe encoding in pupil unit (2, 4 or 6) and

$$\Delta f = \frac{2}{pscale \times isz} \times \frac{180}{\pi} \times 3.6 \cdot 10^6 \times \lambda_0$$

is the width of a monochromatic fringe-peak with  $pscale$  the plate scale (in mas/px),  $isz$  is the number of pixels sampling the interferogram in the space axis and  $\lambda_0$  is the central wavelength.

## 4.2 Results

The simulations were run for H mag spanning from 5 to 12. Each combiner is run 100 times for generating 100 phase masks run for each magnitude in order to have a reliable estimation of the SNR, especially at high magnitudes.

The dark current is converted into counts to be consistent with the empirical relationship between the number of counts and the magnitude by considering a system gain of 1.2 e-/ADU and a quantum efficiency of 0.6.

The empirical relationship is based on measurements made with the PICNIC camera at 750 Hz as discussed above. A linear rescaling of the factor 10189 allows changing the count in function of the QE and the frame rate.

As suggested in the previous sections, both designs have the same integration time, that is one scan for the pupil combiner and incoherent integration.

The results are shown in Figure 4.

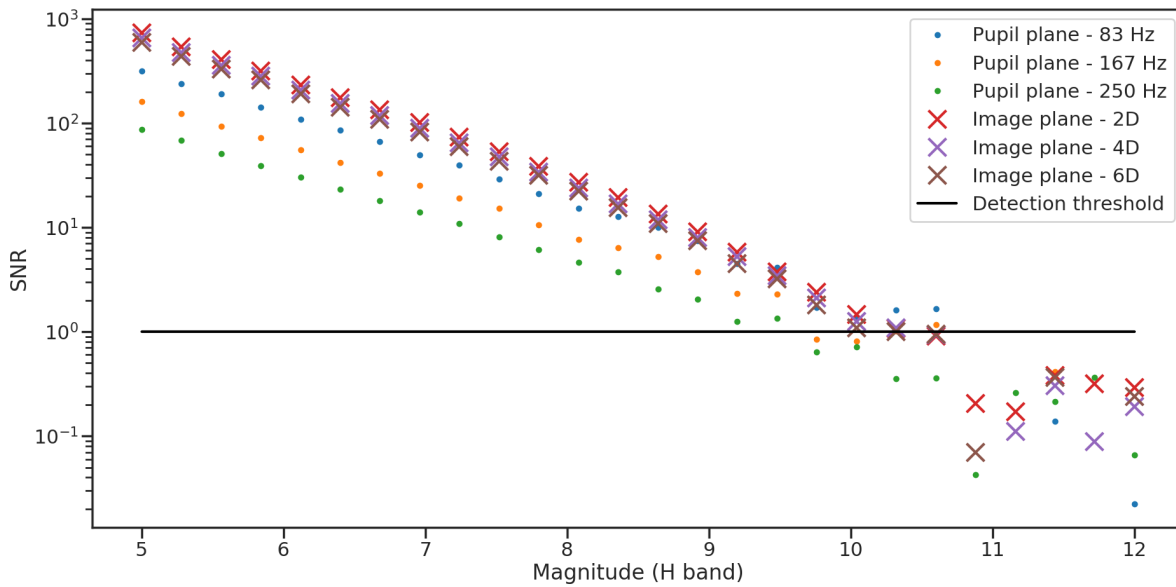


**Figure 4.** The SNR curve for the three baselines in the pupil plane combiner (dots) and image plane combiner (crosses). The detection threshold is set at SNR=1.

## 5 CONCLUSIONS

The primary advantages of the aperture plane design are lower risk, fewer changes to the optical layout, and its ability to scan large amounts of delay space in a relatively short amount of time<sup>2</sup>. The image plane, however, offers the best sensitivity with a gain of nearly one magnitude compared to the pupil plane. Therefore, we can expect a limiting magnitude of 10 in H band with the image plane combiner and about 9 for the worst baseline in the pupil plane combiner. We also note that the SNR is the same for all baselines in the image plane combiner whereas the SNR decreases due to faster fringe encoding in the pupil plane combiner on some baselines. Furthermore, the image plane combiner spends the same amount of time for each baseline which is not the case in the pupil plane combiner. Finally, the image plane design is looking at fringes all the time while the aperture plane systems spends a majority of its scan length away from the center of the fringe packets.

<sup>2</sup> This will be specially important when we try to commission the larger base in the 7<sup>th</sup> telescope project.